

Integration of Polyaniline/Poly(acrylic acid) Films and Redox Enzymes on Electrode Supports: An in Situ Electrochemical/Surface Plasmon Resonance Study of the Bioelectrocatalyzed Oxidation of Glucose or Lactate in the Integrated Bioelectrocatalytic Systems

Oleg A. Raitman,[†] Eugenii Katz,[†] Andreas F. Bückmann,^{‡,§} and Itamar Willner^{*,†}

Contribution from the Institute of Chemistry, The Hebrew University of Jerusalem, Jerusalem 91904, Israel, and Department of Molecular Structure Research, Gesellschaft für Biotechnologische Forschung, Mascheroder Weg 1, D-38124 Braunschweig, Germany

Received December 10, 2001. Revised Manuscript Received February 27, 2002

Abstract: Electropolymerization of aniline in the presence of poly(acrylic acid) on Au electrodes yields a polyaniline/poly(acrylic acid) composite film, exhibiting reversible redox functions in aqueous solutions at pH = 7.0. In situ electrochemical-SPR measurements are used to identify the dynamics of swelling and shrinking of the polymer film upon the oxidation of the polyaniline (PAn) to its oxidized state (PAn²⁺) and the reduction of the oxidized polymer (PAn²⁺) back to its reduced state (PAn), respectively. Covalent attachment of N⁶-(2-aminoethyl)-flavin adenin dinucleotide (amino-FAD, **1**) to the carboxylic groups of the composite polyaniline/poly(acrylic acid) film followed by the reconstitution of apoglucose oxidase on the functional polymer yields an electrically contacted glucose oxidase of unprecedented electrical communication efficiency with the electrode: electron-transfer turnover rate ~1000 s⁻¹ at 30 °C. In situ electrochemical-SPR analyses are used to characterize the bioelectrocatalytic functions of the biomaterial-polymer interface. The current responses of the bioelectrocatalytic system increase as the glucose concentrations are elevated. Similarly, the SPR spectra of the system are controlled by the concentration of glucose. The glucose concentration controls the steady-state concentration ratio of PAn/PAn²⁺ in the film composition. Therefore, the SPR spectrum of the film measured upon its electrochemical oxidation is shifted from the spectrum typical for the oxidized PAn²⁺ at low glucose concentration to the spectrum characteristic of the reduced PAn at high glucose concentration. Similarly, the polyaniline/poly(acrylic acid) film acts as an electrocatalyst for the oxidation of NADH. Accordingly, an integrated bioelectrocatalytic assembly was constructed on the electrode by the covalent attachment of N⁶-(2-aminoethyl)-β-nicotinamide adenine dinucleotide (amino-NAD⁺, **2**) to the polymer film, and the two-dimensional cross-linking of an affinity complex formed between lactate dehydrogenase and the NAD⁺-cofactor units associated with the polymer using glutaric dialdehyde as a cross-linker. In situ electrochemical-SPR measurements are used to characterize the bioelectrocatalytic functions of the system. The amperometric responses of the system increase as the concentrations of lactate are elevated, and an electron-transfer turnover rate of 350 s⁻¹ between the biocatalyst and the electrode is estimated. As the PAn²⁺ oxidizes the NADH units generated by the biocatalyzed oxidation of lactate, the PAn/PAn²⁺ steady-state ratio in the film is controlled by the concentration of lactate. Accordingly, the SPR spectrum measured upon electrochemical oxidation of the film is similar to the spectrum of PAn²⁺ at low lactate concentration, whereas the SPR spectrum resembles that of PAn at high concentrations of lactate.

Introduction

Thin-film assemblies organized on electrode supports represent important functional elements in various electronic and optical devices such as photoelectrochemical cells,¹ light-emitting diodes,² conductive polymer-based batteries,³ electrochromic windows,⁴ signal-triggered actuators,⁵ optoelectronic

systems,⁶ and bioelectrochemical⁷ and optobioelectronic⁸ assemblies. Surface plasmon resonance spectroscopy (SPR) is an

* To whom correspondence should be addressed. E-mail: willnea@vms.huji.ac.il. Tel: 972-2-6585272. Fax: 972-2-6527715.

[†] The Hebrew University of Jerusalem.

[‡] Gesellschaft für Biotechnologische Forschung.

[§] Deceased, October 2001.

- (1) (a) Cao, T. B.; Yang, S. M.; Yang, Y.L.; Huang, C. H.; Cao, W. X. *Langmuir* **2001**, *17*, 6034–6036. (b) Oekermann, T.; Yoshida, T.; Schlettwein, D.; Sugiura, T.; Minoura, H. *Phys. Chem. Chem. Phys.* **2001**, *3*, 3387–3392. (c) Willner, I.; Willner, B. *Pure Appl. Chem.* **2001**, *73*, 535–542.
- (2) (a) Mitschke, U.; Bäuerle, P. *J. Mater. Chem.* **2000**, *10*, 1471–1507. (b) Kalinowski, D. *J. Phys. D Appl. Phys.* **1999**, *32*, R179–R249.
- (3) (a) MacDiarmid, A. G.; Mu, S. L.; Somasiri, N. L. D.; Mu, W. *Mol. Cryst. Liq. Cryst.* **1985**, *121*, 187–195. (b) Meyer, W. H. *Adv. Mater.* **1998**, *10*, 439–448.
- (4) Bechinger, C.; Ferrer, S.; Zaban, A.; Sprague, J.; Gregg, B. A. *Nature* **1996**, *383*, 608–610.

effective spectroscopic method to characterize the optical and structural (thickness) features of thin-film assemblies.⁹ Usually, these parameters are derived by the theoretical fitting of the experimental reflectance spectra using the Fresnel equation.^{10,11} SPR spectroscopy has been widely applied to characterize protein and enzyme thin films on surfaces,^{12,13} biorecognition binding processes on Au supports,^{14,15} and chemical transformations on surfaces.^{16,17} In situ electrochemical-SPR measurements provide an effective method to characterize structural or optical properties of redox-activated interfaces on gold supports.¹⁸ Indeed, in situ electrochemical-SPR experiments on redox-activated polymer films were used to follow swelling/shrinking processes of polymers¹⁹ and ion migration in charged polymers²⁰ and for the determination of the optical properties of polymer films.²¹

The assembly of biomaterials as monolayer or multilayer films on surfaces is the subject of extensive recent research efforts directed to the development of biosensors,^{22,23} biofuel cells,²⁴ and optobioelectronic systems.²⁵ Immobilization of redox enzymes on electrodes, and the electrochemical activation of the biocatalysts, is a common practice to develop amperometric

biosensors.^{22,23} Redox enzymes usually lack direct electrical communication with electrode supports. The application of diffusional electron mediators,²⁶ the tethering of redox relay groups to the enzyme,^{27,28} the encapsulation of the biocatalysts in redox polymers,²⁹ or the surface reconstitution of redox apoenzymes on relay cofactor units³⁰ provide, however, general routes to electrically communicate with the redox enzymes and the electrodes. Conductive polymers and polymers functionalized with redox units have been applied as wiring matrixes for the electrochemical activation of redox enzymes.³¹ For example, an Os complex-containing polymer provides an oxidative electron path from the entrapped glucose oxidase,^{31a} whereas a bipyridinium-containing polymer allows reductive electron transfer to the nitrate reductase enzyme.^{31d}

Thus, the integration of redox enzymes with redox polymers as mediating electron-transfer units at Au surfaces would enable the in situ electrochemical-SPR transduction of the bioelectrocatalytic processes. Only a few examples of in situ electrochemical-SPR measurements in the presence of redox proteins are available. These include the characterization of electron transfer of cytochrome *c* at a monolayer-modified electrode,^{12b} and the polyaniline-mediated reduction of H₂O₂ in the presence of horseradish peroxidase.^{13a} Here we report on the organization of integrated, electrically contacted, films consisting of polyaniline/poly(acrylic acid) modified with glucose oxidase (GOx) or polyaniline/poly(acrylic acid) modified with the NAD⁺-dependent lactate dehydrogenase (LDH) on Au supports. We characterize the systems by in situ electrochemical-SPR measurements. We demonstrate that surface plasmon resonance spectroscopy may be employed as a method complementary to electrochemistry to transduce bioelectrocatalytic transformations. In the different systems, we emphasize the nanoengineering elements that include the tailored integration of the enzymes with the conductive polymer in order to achieve effective electrical contact.

Experimental Section

Chemicals. N⁶-(2-Aminoethyl)-flavin adenin dinucleotide³² (amino-FAD, **1**) and N⁶-(2-aminoethyl)-β-nicotinamide adenine dinucleotide³³ (amino-NAD⁺, **2**) were synthesized and purified as described before.

- (5) (a) Raiteri, R.; Grattarola, M.; Butt, H.-J.; Skládal, P. *Sens. Actuators, B* **2001**, *79*, 115–126. (b) Lahav, M.; Durkan, C.; Gabai, R.; Katz, E.; Willner, I.; Welland, M. E. *Angew. Chem., Int. Ed.* **2001**, *40*, 4095–4097.
- (6) (a) Shipway, A. N.; Willner, I. *Acc. Chem. Res.* **2001**, *34*, 421–432. (b) Willner, I.; Doron, A.; Katz, E. *J. Phys. Org. Chem.* **1998**, *11*, 546–560.
- (7) (a) Willner, I.; Katz, E. *Angew. Chem., Int. Ed.* **2000**, *39*, 1180–1218. (b) Heller, A. *Acc. Chem. Res.* **1990**, *23*, 128–134. (c) Habermüller, L.; Mosbach, M.; Schuhmann, W. *Fresenius J. Anal. Chem.* **2000**, *366*, 560–568.
- (8) Willner, I.; Rubin, S. *Angew. Chem., Int. Ed. Engl.* **1996**, *35*, 367–385.
- (9) (a) Knoll, W. *Annu. Rev. Phys. Chem.* **1998**, *49*, 569–638. (b) Badia, A.; Arnold, S.; Scheumann, V.; Zitzler, M.; Mack, J.; Jung, G.; Knoll, W. *Sens. Actuators, B* **1999**, *54*, 145–165. (c) Homola, J.; Yee, S. S.; Gauglitz, G. *Sens. Actuators, B* **1999**, *54*, 3–15.
- (10) (a) Sadowski, J. W.; Korhonen, I. K. J.; Peltonen, J. P. K. *Opt. Eng.* **1995**, *34*, 2581–2586. (b) Johnston, K. S.; Karlens, S. R.; Jung, C. C.; Yee, S. S. *Mater. Chem. Phys.* **1995**, *42*, 242–246.
- (11) Beketov, G. V.; Shirshov, Y. M.; Shynkarenko, O. V.; Chegel, V. I. *Sens. Actuators, B* **1998**, *48*, 432–438.
- (12) (a) Schlereth, D. D.; Kooyman, R. P. H. *J. Electroanal. Chem.* **1998**, *444*, 231–240. (b) Schlereth, D. D. *J. Electroanal. Chem.* **1999**, *464*, 198–207.
- (13) (a) Iwasaki, Y.; Horiuchi, T.; Niwa, O. *Anal. Chem.* **2001**, *73*, 1595–1598. (b) Salamon, Z.; Macleod, H. A.; Tollin, G. *Biochim. Biophys. Acta* **1997**, *1331*, 117–129.
- (14) (a) Rao, J.; Yan, L.; Xu, B.; Whitesides, G. M. *J. Am. Chem. Soc.* **1999**, *121*, 2629–2630. (b) Sasaki, S.; Nagata, R.; Hock, B.; Karube, I. *Anal. Chim. Acta* **1998**, *368*, 71–76. (c) Berger, C. E. H.; Greve, J. *Sens. Actuators, B* **2000**, *63*, 103–108.
- (15) (a) Mullett, W. M.; Lai, E. P. C.; Yeung, J. M. *Methods* **2000**, *22*, 77–91. (b) Disley, D. M.; Cullen, D. C.; You, H. X.; Lowe, C. R. *Biosens. Bioelectron.* **1998**, *13*, 1213–1225. (c) Kruchinin, A. A.; Vlasov, Y. G. *Sens. Actuators, B* **1996**, *30*, 77–80. (d) McDonnell, J. M. *Curr. Opin. Chem. Biol.* **2001**, *5*, 572–577.
- (16) (a) Georgiadis, R.; Peterlinz, K. A.; Rahn, J. R.; Peterson, A. W.; Grassi, J. H. *Langmuir* **2000**, *16*, 6759–6762. (b) Tsoi, P. Y.; Yang, J.; Sun, Y.; Sui, S.; Yang, M. *Langmuir* **2000**, *16*, 6590–6596. (c) Ehler, T. T.; Walker, J. W.; Jurchen, J.; Shen, Y.; Morris, K.; Sullivan, B. P.; Noe, L. J. *J. Electroanal. Chem.* **2000**, *480*, 94–100.
- (17) (a) Sota, H.; Hasegawa, Y.; Iwakura, M. *Anal. Chem.* **1998**, *70*, 2019–2024. (b) Kienle, S.; Lingler, S.; Kraus, W.; Offenhausser, A.; Knoll, W.; Jung, G. *Biosens. Bioelectron.* **1997**, *12*, 779–786. (c) Flatmark, T.; Stokka, A. J.; Berge, S. V. *Anal. Biochem.* **2001**, *294*, 95–101.
- (18) (a) Yan, J. C.; Tender, L. M.; Hampton, P. D.; Lopez, G. P. *J. Phys. Chem. B* **2001**, *105*, 8905–8910. (b) Kang, X. F.; Cheng, G. J.; Dong, S. J.; *Electrochem. Commun.* **2001**, *3*, 489–493.
- (19) Chegel, V.; Raitman, O.; Katz, E.; Gabai, R.; Willner, I. *Chem. Commun.* **2001**, 883–884.
- (20) Brennan, C. B.; Sun, L. F.; Weber, S. G. *Sens. Actuators, B* **2001**, *72*, 1–10.
- (21) Kambhampati, D. K.; Knoll, W. *Curr. Opin. Colloid Interface Sci.* **1999**, *4*, 273–280.
- (22) (a) Schmidt, H.-L.; Schuhmann, W. *Biosens. Bioelectron.* **1996**, *11*, 127–135. (b) Kuwabata, S.; Okamoto, T.; Kajiyama, Y.; Yoneyama, H. *Anal. Chem.* **1995**, *67*, 1684–1690. (c) Jin, W.; Bier, F.; Wollenberger, U.; Scheller, F. *Biosens. Bioelectron.* **1995**, *10*, 823–829.
- (23) (a) Willner, I.; Riklin, A.; Shoham, B.; Rivenson, D.; Katz, E. *Adv. Mater.* **1993**, *5*, 912–915. (b) Willner, I.; Katz, E.; Willner, B. *Electroanalysis* **1997**, *9*, 965–977.
- (24) (a) Willner, I.; Katz, E.; Patolsky, F.; Bückmann, A. F. *J. Chem. Soc., Perkin Trans. 2* **1998**, 1817–1822. (b) Katz, E.; Filanovsky, B.; Willner, I. *New J. Chem.* **1999**, *23*, 481–487. (c) Katz, E.; Willner, I.; Kotlyar, A. B. *J. Electroanal. Chem.* **1999**, *479*, 64–68. (d) Katz, E.; Shipway, A. N.; Willner, I. In *Handbook of Fuel Cell Technology*; Vielstich, W., Gasteiger, H., Lamm, A., Eds.; Wiley: New York, in press.
- (25) (a) Willner, I.; Katz, E.; Willner, B.; Blonder, R.; Heleg-Shabtai, V.; Bückmann, A. F. *Biosens. Bioelectron.* **1997**, *12*, 337–356. (b) Blonder, R.; Katz, E.; Willner, I.; Wray, V.; Bückmann, A. F. *J. Am. Chem. Soc.* **1997**, *119*, 11747–11757.
- (26) Bartlett, P. N.; Tebbutt, P.; Whitaker, R. G. *Prog. React. Kinet.* **1991**, *16*, 55–155.
- (27) (a) Degani, Y.; Heller, A. *J. Phys. Chem.* **1987**, *91*, 1285–1289. (b) Degani, Y.; Heller, A. *J. Am. Chem. Soc.* **1988**, *110*, 2615–2620. (c) Schuhmann, W.; Ohara, T. J.; Schmidt, H.-L.; Heller, A. *J. Am. Chem. Soc.* **1991**, *113*, 1394–1397. (d) Badia, A.; Carlini, R.; Fernandez, A.; Battagliani, F.; Mikkelsen, S. R.; English, A. M. *J. Am. Chem. Soc.* **1993**, *115*, 7053–7060.
- (28) (a) Willner, I.; Katz, E.; Riklin, A.; Kahser, R. *J. Am. Chem. Soc.* **1992**, *114*, 10965–10966. (b) Willner, I.; Lapidot, N.; Riklin, A.; Kasher, R.; Zahavy, E.; Katz, E. *J. Am. Chem. Soc.* **1994**, *116*, 1428–1441.
- (29) Emr, S. A.; Yacynych, A. M. *Electroanalysis* **1995**, *7*, 913–923.
- (30) (a) Willner, I.; Heleg-Shabtai, V.; Blonder, R.; Katz, E.; Tao, G.; Bückmann, A. F.; Heller, A. *J. Am. Chem. Soc.* **1996**, *118*, 10321–10322. (b) Katz, E.; Riklin, A.; Heleg-Shabtai, V.; Willner, I.; Bückmann, A. F. *Anal. Chim. Acta* **1999**, *385*, 45–58.
- (31) (a) Gregg, B. A.; Heller, A. *J. Phys. Chem.* **1991**, *95*, 5970–5975. (b) Koide, S.; Yokoyama, K. *J. Electroanal. Chem.* **1999**, *468*, 193–201. (c) Cosnier, S.; Decout, J.-L.; Fontecave, M.; Frier, C.; Innocent, C. *Electroanalysis* **1998**, *10*, 521–525. (d) Cosnier, S.; Innocent, C.; Jouanneau, Y. *Anal. Chem.* **1994**, *66*, 3198–3201.

Lactate dehydrogenase (LDH, EC 1.1.1.27 from rabbit muscle, type II) and glucose oxidase (GOx, EC 1.1.3.4 from *Aspergillus niger*) were purchased from Sigma and used without further purification. Apogluco oxidase (apo-GOx) was prepared by a modification^{30b} of a reported method.³⁴ All other chemicals, including 1,4-dihydro- β -nicotinamide adenine dinucleotide (NADH, **3**), 4-(2-hydroxyethyl)piperazine-1-ethanesulfonic acid sodium salt (HEPES), 1-ethyl-3-(3-dimethylaminopropyl)carbodiimide (EDC), aniline, glutaric dialdehyde, poly(acrylic acid) (450 000 g·mol⁻¹), glucose, and lactate were purchased from Aldrich or Sigma and used as supplied. Ultrapure water from Serapur Pro 90 CN source was used in all experiments.

In Situ Electrochemical-SPR Measurements. The SPR Kretschmann-type spectrometer Biosuplar-2 (Analytical- μ System; light-emitting diode light source, $\lambda = 670$ nm) was used in this work. A high refraction index of the prism ($N = 1.61$) and a broad dynamic diapason (up to 19° in air) of the SPR instrument allowed the SPR analyses of thick polymer films (up to 200 nm) without change of the initial angle. This is an important condition for the correctness of the computer fitting of the experimental data to a theoretical curve. The SPR data were processed using Biosuplar-2 software (version 2.2.30) on a PC computer. The experimental SPR spectra of the polymer film were fitted to the theoretical curves based on five-phase Fresnel calculations using the Nelder–Mead algorithm of minimization.¹¹

Cyclic voltammetry and multipotential step chronoamperometry experiments were performed using an electrochemical analyzer (EG&G, VersaStat) linked to a computer (EG&G software 270/250). The use of a simple open cell (230 μ L) enabled easy emptying of the cell contents and thus rapid removal and change of solution above the polymer films when needed. Glass supports (TF-1 glass, 20 \times 20 mm) covered with a Cr thin sublayer (5 nm) and a polycrystalline Au layer (50 nm) supplied by Analytical- μ System were used for the in situ electrochemical-SPR measurements. The Au-covered glass plate was used as a working electrode (1.5-cm² area exposed to the solution); an auxiliary Pt and a quasi-reference Ag electrodes were made from wires of 0.5-mm diameter and added to the cell. The Ag quasi-reference electrode was calibrated³⁵ according to the potential of dimethyl viologen, $E^\circ = -0.687$ V versus SCE, measured by cyclic voltammetry, and the potentials are reported versus SCE. The SPR sensograms (time-dependent changes of the reflectance minimum) were measured in situ upon application of an external potential onto the working electrode.

Modification of Au Electrodes with Polyaniline/Poly(acrylic acid) Composites and the Assembly of the Integrated Enzyme/Cofactor/Redox Polymer Films on Electrodes. A polyaniline/poly(acrylic acid) composite layer was generated on a Au-coated glass support by the electropolymerization of aniline, 0.2 M, in an electrolyte solution, pH = 1.8, composed of 0.1 M H₂SO₄ and 0.5 M Na₂SO₄, that included poly(acrylic acid) (450 000 g·mol⁻¹), 15 mg·mL⁻¹.³⁶ The polymerization was performed by the application of one potential cycle between -0.1 and +1.1 V, potential scan rate of 100 mV·s⁻¹. The resulting film was washed with the background electrolyte solution composed of 0.1 M H₂SO₄ and 0.5 M Na₂SO₄ to exclude any residual monomer from the cell.

The covalent coupling of amino-FAD (**1**) to the polyaniline/poly(acrylic acid)-modified Au electrode was performed by soaking the electrode in a 0.01 M HEPES buffer solution, pH = 7.2, that includes **1**, 5 \times 10⁻⁴ M, and EDC, 1 \times 10⁻³ M, for 2 h at room temperature. The resulting electrode was washed with 0.1 M phosphate buffer, pH = 7.0, to remove nonreacted **1**. The electrode functionalized with the

FAD-modified polymer film was incubated in a 0.1 M phosphate buffer solution, pH = 7.0, that included the apo-GOx, 1 mg mL⁻¹, for 5 h at room temperature. The resulting electrode was washed with the phosphate buffer to remove any unbound apo-GOx.

The covalent coupling of amino-NAD⁺ (**2**) to the polyaniline/poly(acrylic acid)-modified Au electrode was performed by soaking the polymer-functionalized electrode in the 0.01 M HEPES buffer solution, pH = 7.2, that includes **2**, 5 \times 10⁻⁴ M, and EDC, 1 \times 10⁻³ M, for 2 h at room temperature. The resulting electrode was washed with the 0.1 M phosphate buffer solution, pH = 7.0, to remove any unreacted **2**. The electrode functionalized with the NAD⁺-modified polymer was incubated in 0.1 M phosphate buffer, pH = 7.0, that included LDH, 1 mg mL⁻¹, for 10 min. Then the electrode was briefly (1 s) washed with the phosphate buffer solution and immediately immersed in the solution of glutaric dialdehyde, 10% (v/v) in 0.1 M phosphate buffer, pH = 7.0, for 10 min. After the cross-linking of LDH, the electrode surface was washed with phosphate buffer to remove any unbound LDH.

All the steps of the electrode modification including electrochemical deposition of the composite polymer layer and assembling of cofactor/enzyme units were performed in the SPR electrochemical cell, and the SPR spectra were measured after each reaction step to follow the Au electrode modification. All modification steps and measurements were performed in air at ambient temperature, ~ 30 °C.

Microgravimetric, Quartz-Crystal Microbalance (QCM) Measurements. A QCM analyzer (Fluke 164T multifunction counter, 1.3 GHz, TCXO) and quartz crystals (AT-cut, 9 MHz, Seiko) sandwiched between two Au electrodes (area 0.196 cm², roughness factor ~ 3.5) were employed for the microgravimetric analyses in air. The QCM crystals were calibrated by electropolymerization of aniline in 0.1 M H₂SO₄ and 0.5 M Na₂SO₄ electrolyte solution, followed by coulometric assay of the resulting PAn film and relating of the crystal frequency changes to the electrochemically derived polymer mass.

Results and Discussion

The conductive polymer employed in our studies is polyaniline (PAn). This polymer is, however, redox-active only in acidic solutions,³⁷ pH < 3, thus preventing its integration with redox enzymes that usually operate in neutral pH regions. It was reported, however, that composite polyaniline polymers doped with poly(vinyl sulfonate)³⁸ or poly(acrylic acid),³⁶ switch the redox activity of the polyaniline to neutral pH regions. Accordingly, aniline was electropolymerized on Au electrodes in the presence of poly(acrylic acid) (Scheme 1). The composite polymer layer was prepared by one voltammetric cycle where the potential was swept from -0.1 to 1.1 V and back, scan rate 100 mV·s⁻¹. Figure 1 shows the cyclic voltammogram of the resulting polymer layer, at pH = 7.0. It shows a quasi-reversible electrochemical process of the redox polymer-modified Au electrode, with a peak-to-peak separation of 85 mV at the potential scan rate 100 mV·s⁻¹. By coulometric assay of the oxidation (or reduction) wave of PAn, $E^\circ = 0.29$ V, the surface coverage of polyaniline is estimated to be $\sim 9.3 \times 10^{-8}$ g·cm⁻². The Figure 1 inset shows the SPR spectrum of the resulting composite polyaniline/poly(acrylic acid) film in water (curve a), and the theoretical fit (curve b) according to the Fresnel

(32) Bückmann, A. F.; Wray, V.; Stocker, A. In *Methods in Enzymology: Vitamins and Coenzymes*; McCormick, D. B., Ed.; Academic Press: Orlando, FL, 1997; Vol. 280, Part 1, p 360.

(33) Bückmann, A. F.; Wray, V. *Biotech. Appl. Biochem.* **1992**, *15*, 303–310.

(34) Morris, D. L.; Buckler, R. T. In *Methods in Enzymology*; Langone, J. J., Van Vunakis, H., Eds.; Academic Press: Orlando, FL, 1983; Vol. 92, Part E, pp 413–417.

(35) Katz, E.; Schlereth, D. D.; Schmidt, H.-L. *J. Electroanal. Chem.* **1994**, *367*, 59–70.

(36) Bartlett, P. N.; Simon, E. *Phys. Chem. Chem. Phys.* **2000**, *2*, 2599–2606.

(37) (a) Ohsaka, T.; Ohnuki, Y.; Oyama, N.; Katagiri, K.; Kamisako, K. *J. Electroanal. Chem.* **1984**, *161*, 399–405. (b) Diaz, A. F.; Logan, J. A. *J. Electroanal. Chem.* **1980**, *111*, 111–114. (c) Cui, S. Y.; Park, S. M. *Synth. Met.* **1999**, *105*, 91–98. (d) Jannakoudakis, P. D.; Pagalos, N. *Synth. Met.* **1994**, *68*, 17–31.

(38) (a) Bartlett, P. N.; Wang, J. H. *J. Chem. Soc., Faraday Trans.* **1996**, *92*, 4137–4143. (b) Bartlett, P. N.; Birkin, P. R.; Wallace, E. N. K. *J. Chem. Soc., Faraday Trans.* **1997**, *93*, 1951–1960. (c) Bartlett, P. N.; Wallace, E. N. K. *Phys. Chem. Chem. Phys.* **2001**, *3*, 1491–1496.

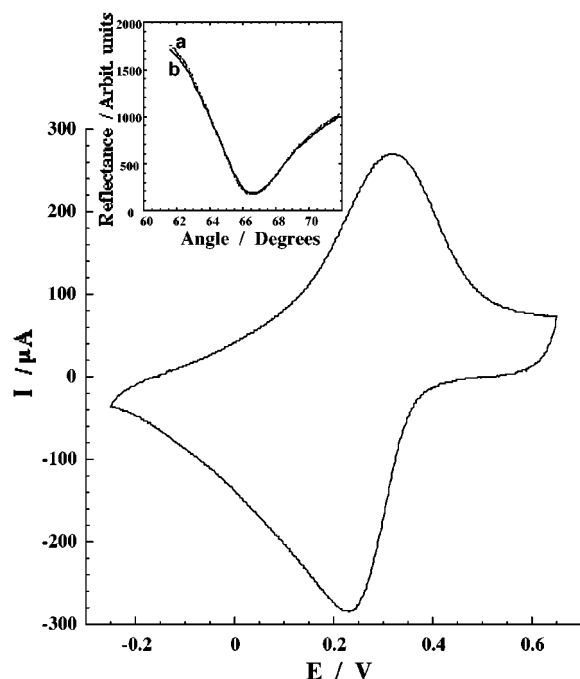
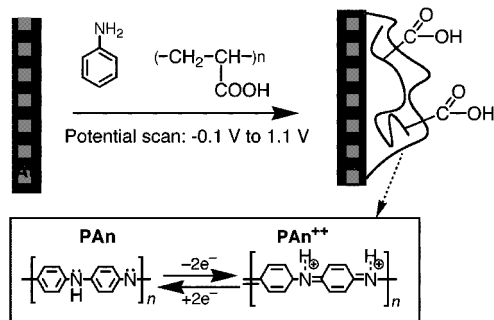


Figure 1. Cyclic voltammogram of a polyaniline/poly(acrylic acid) film-functionalized Au electrode recorded in 0.1 M phosphate buffer, pH = 7.0, potential scan rate, $100 \text{ mV}\cdot\text{s}^{-1}$. Inset: The SPR spectrum of the respective polyaniline/poly(acrylic acid) film-functionalized Au electrode recorded in water (a) and its theoretical fitting (b).

Scheme 1. Modification of a Au Electrode with a Composite Redox Polymer Film Consisting of Polyaniline and Poly(acrylic acid)



equation ($n = 1.4$ used for the first approximation³⁹ and $n = 1.393 + 0.04j$ received after the fitting), implying that the composite PAn/poly(acrylic acid) film does not differ substantially in its refractive index from pure PAn and that the film is uniform. The polymer layer thickness derived from the SPR spectrum fitting is 90 nm.

Figure 2, curves a and b, shows the SPR spectra of the reduced polyaniline state (PAn) generated upon application of a potential corresponding to -0.3 V and that of the oxidized polyaniline state (PAn^{2+}) generated upon the application of a potential of 0.6 V on the electrode, respectively. The change in the SPR spectrum upon the oxidation of PAn to PAn^{2+} is attributed to a change in the refraction index of the polymer upon oxidation (vide infra). Application of sequential potential steps on the polyaniline/poly(acrylic acid)-modified electrode, where the potential is stepped from -0.3 V (PAn state) to $+0.6 \text{ V}$ (PAn^{2+} state) and back (the electrode is maintained at each

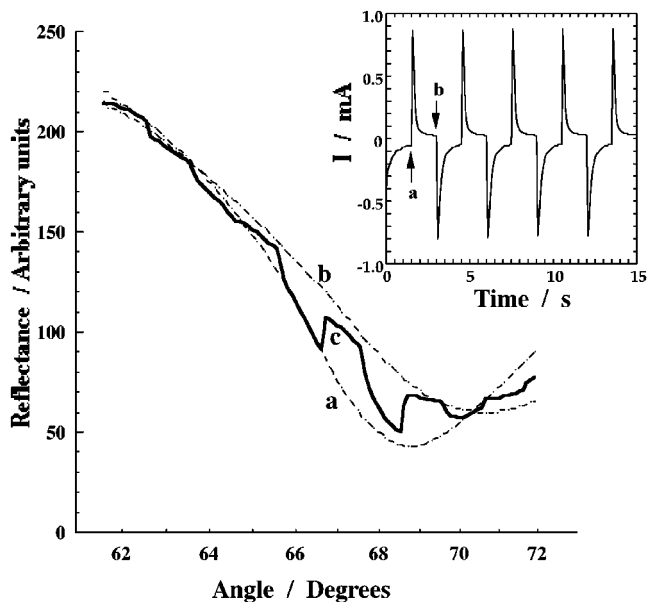


Figure 2. SPR spectra of a polyaniline/poly(acrylic acid) thin film-functionalized Au electrode recorded at different applied potentials: (a) At $E = -0.3 \text{ V}$. (b) At $E = 0.6 \text{ V}$. (c) The potential is stepped between -0.3 and 0.6 V and back with time intervals of 1.5 s . Inset: Chronoamperometric measurements with the potential steps between 0.6 V (a) and -0.3 V (b) with time intervals of 1.5 s between the potential steps.

potential for 1.5 s) results in the chronoamperometric transients shown in Figure 2 (inset). Concomitantly, the surface plasmon spectrum of the film is cycled between the spectra of oxidized and reduced states of the polymer, Figure 2, curve c. Figure 3A shows the time-dependent reflectance changes in the SPR spectra at a fixed angle of incidence ($\phi = 67.5^\circ$), as a result of the potential multistep sequence applied to the modified electrode (Figure 3B). (Note that the oxidation or reduction steps are applied for 20 s , which is a substantially longer time interval than that in Figure 2, inset.) Oxidation of the polymer film from PAn to PAn^{2+} results in a rapid change in the reflectance intensity, followed by a slow increase in the reflectance. Similarly, the reduction of PAn^{2+} to PAn results in a fast, instantaneous, decrease in the reflectance intensity followed by a slow decrease in the reflectance intensity. The fast increase in the SPR reflectance upon the oxidation of PAn to PAn^{2+} is attributed to a change in the refractive index of the polymer film as a result of its oxidation. The slow increase in the reflectance intensity observed upon the oxidation of the polymer is attributed to the swelling of the oxidized polymer. The swelling is attributed to the uptake of counteranions, accompanied by the hydration of the polymer. Similarly, the fast decrease in the reflectance intensity observed upon the reduction of PAn^{2+} is attributed to the restoration of the refractive index of PAn. The slow decrease in the reflectance intensity is then attributed to the shrinking of the reduced polymer as a result of the release of counteranions and dehydration of the film.¹⁹ Theoretical fitting of the SPR spectrum obtained immediately after oxidation to PAn^{2+} , and assuming that the oxidized polymer thickness is identical to the PAn thickness (90 nm , as the polymer does not swell within this time interval) yields a refractive index value of $n = 1.389 + 0.47j$. Theoretical fitting of the SPR spectrum of PAn^{2+} after reaching the saturated swollen configuration, using the derived value of the refractive index for PAn^{2+} , yields a polymer thickness of 120 nm for the

(39) Mo, D.; Lin, Y. Y.; Tan, J. H.; Yu, Z. X.; Zhou, G. Z.; Gong, K. C.; Zhang, G. P.; He, X.-F. *Thin Solid Films* **1993**, *234*, 468–470.

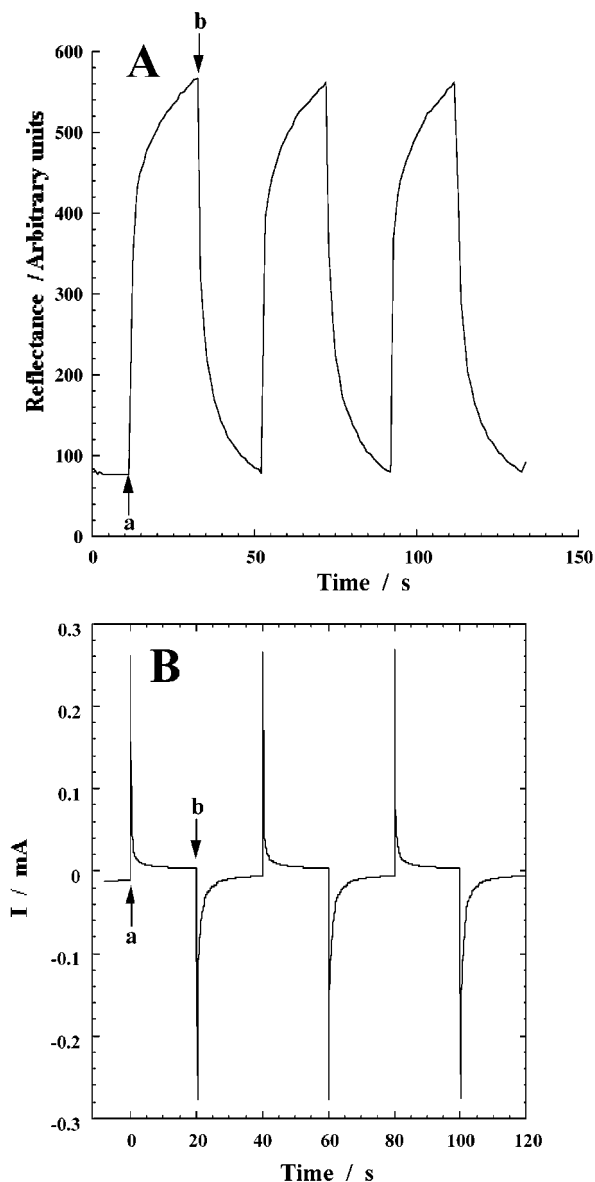


Figure 3. (A) Time-dependent reflectance changes of the polyaniline/poly(acrylic acid) thin-film-functionalized Au electrode measured at a fixed angle of incidence ($\phi = 67.5^\circ$) upon the application of multistep potential cycles. (B) Chronoamperometric transients corresponding to the SPR spectra in (A), generated by potential steps between -0.3 and 0.6 V and back with time intervals of 20 s between the potential steps. The arrows show the time of the application of the oxidative potential, 0.6 V, (a), and reductive potential, -0.3 V, (b), respectively. The chronoamperometric and in situ SPR measurements were performed in 0.1 M phosphate buffer, $\text{pH} = 0.7$.

swollen PAN^{2+} . Thus, the polymer thickness increases by 30 nm because of the swelling process induced by polymer oxidation. In turn, theoretical fitting of the SPR spectrum of the PAN film obtained immediately after reduction of PAN^{2+} to PAN yields a polymer thickness of 120 nm that corresponds to the swollen assembly. Theoretical fitting of the SPR spectrum obtained after relaxation of the reduced polymer yields the original polymer thickness of 90 nm. This means full reversibility of the swelling–shrinking processes induced by the cyclic potential changes between -0.3 and 0.6 V. Kinetic analyses of the time-dependent increase in the reflectance intensity yields a swelling rate constant that corresponds to $k_{\text{swell}} = 3.5 \times 10^{-4} \text{ s}^{-1}$ and a shrinking rate constant of $k_{\text{shrink}} = 2.2 \times 10^{-4} \text{ s}^{-1}$ for

the oxidized and reduced polymer films, respectively. These rate constants of the composite polyaniline/poly(acrylic acid) film measured at $\text{pH} = 7.0$ are very similar to those reported previously for a polyaniline film¹⁹ in an acidic solution, $\text{pH} = 1.8$. The SPR reflectance intensity can be reversibly switched between high- and low-intensity values upon the electrochemical cycling of the polymer film between the PAN^{2+} and PAN states, respectively. Thus, the system represents an electrochemical switch where optical SPR transduction provides the read-out signal of the “ON”/“OFF” states of the polymer film.

The fact that the polyaniline polymer exhibits redox activity at $\text{pH} = 7.0$, as a result of the incorporation of poly(acrylic acid), suggests that one could integrate biocatalysts with the polymer film on the electrodes. Furthermore, the carboxylic acid residues of the poly(acrylic acid) component could provide sites for covalent tethering of biocatalysts to the polymer. Thus, the bioelectrocatalytic functions of the PAN/enzyme electrode could then be transduced by in situ electrochemical-SPR experiments.

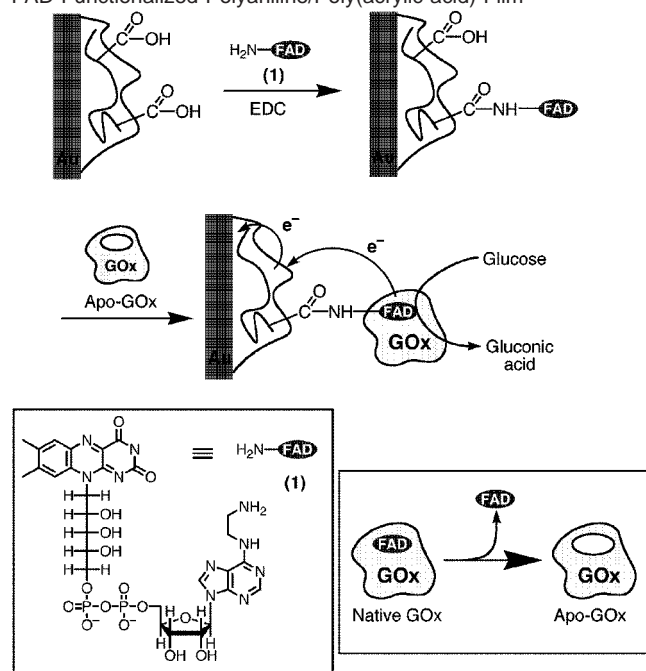
In situ electrochemical-SPR measurements were applied to characterize the bioelectrocatalyzed oxidation of glucose by a composite polyaniline/poly(acrylic acid) film that includes an engineered glucose oxidase. Our laboratory has demonstrated that reconstitution of apoglucose oxidase on a relay-FAD monolayer yields a biocatalyst of unprecedented electrical contact efficiency with the electrode.³⁰ This extremely efficient electrical communication between the biocatalyst redox site and the electrode was attributed to the structural alignment of the redox biocatalyst on the electrode surface, in a configuration that provides a directional electron wiring between the enzyme redox site and the conducting support. The fact that a polyaniline film can activate redox enzymes such as glucose oxidase or horseradish peroxidase⁴⁰ suggests that appropriate immobilization of GOx in the polyaniline film could lead to an integrated electrically contacted bioelectrocatalytic assembly for the oxidation of glucose. Scheme 2 outlines the method we employed to construct the integrated polyaniline/poly(acrylic acid)/GOx bioelectrocatalytic film on the electrode surface. The polyaniline/poly(acrylic acid) film is functionalized with the flavin cofactor by the covalent coupling of amino-FAD to the carboxylic acid residues of poly(acrylic acid). Reconstitution of apoglucose oxidase on the FAD units yields the bioelectrocatalytic redox-active polymer film.

Complementary microgravimetric, QCM measurements were performed on Au–quartz crystals functionalized with the polyaniline/poly(acrylic acid) film. The polymer film on the Au–quartz crystals was generated by the same procedure as employed for the modification of the Au–SPR electrodes. The changes in the quartz-crystal resonance frequencies were measured in air upon the electropolymerization step, after covalent coupling of the amino-FAD and, subsequently, after the reconstitution of GOx on the FAD-functionalized film. From the frequency changes, and using the Sauerbrey relation,⁴¹ the mass changes on the electrode as a result of the formation of the polymer film, the further covalent binding of the FAD units, and the surface reconstitution of GOx were calculated. The composite polymer film coverage of $1.27 \times 10^{-7} \text{ g}\cdot\text{cm}^{-2}$ was de-

(40) (a) Bartlett, N. P.; Birkin, P. R. *Anal. Chem.* **1993**, *66*, 1118–1119. (b) Bartlett, N. P.; Birkin, P. R. *Anal. Chem.* **1994**, *66*, 1552–1559. (c) Bartlett, N. P.; Birkin, P. R.; Palmisano, F.; DeBenedetto, G. *J. Chem. Soc., Faraday Trans.* **1996**, *92*, 3123–3130.

(41) Buttry, D. A.; Ward, M. D. *Chem. Rev.* **1992**, *92*, 1355–1379.

Scheme 2. Reconstitution of Glucose Oxidase (GOx) on the FAD-Functionalized Polyaniline/Poly(acrylic acid) Film



rived from the frequency change after the electropolymerization. Taking into account the electrode coverage with the redox-active polyaniline component, $9.3 \times 10^{-8} \text{ g}\cdot\text{cm}^{-2}$, derived from the coulometric measurements, we estimated that the electrochemically inactive poly(acrylic acid) component has a coverage of $3.4 \times 10^{-8} \text{ g}\cdot\text{cm}^{-2}$ that is 27% (w/w) of the composite polymer film. Assuming that the polyaniline/poly(acrylic acid) film density⁴² is $\sim 1.1\text{--}1.2 \text{ g}\cdot\text{mL}^{-1}$ and that the homogeneous electrodeposition of the polymer film occurs on the surface, we estimate the thickness of the polymer film to be $\sim 100 \text{ nm}$. This value is similar to the polymer thickness of 90 nm derived from the fitting of the SPR spectrum.

Knowing the masses of the immobilized **1** and the surface-reconstituted GOx and the area of the Au-quartz crystal, the surface coverages of **1** and GOx on the polymer film were calculated to be $\sim 2 \times 10^{-11}$ and $\sim 3 \times 10^{-12} \text{ mol}\cdot\text{cm}^{-2}$, respectively. Using the footprint dimension of GOx (58 nm^2),⁴³ and the calculated surface coverage of GOx on the electrode, we find that the enzyme coverage corresponding to a densely packed enzyme monolayer is formed on the polymer film. Since the thickness of the electrochemically polymerized films on the SPR electrodes and Au-quartz crystals are similar, we assume that similar coverages of the biocatalyst are obtained on the SPR electrodes.

Figure 4A shows the cyclic voltammograms of the polyaniline/poly(acrylic acid)/GOx film-functionalized electrode in the presence of various concentrations of glucose. As the concentration of glucose increases, the electrocatalytic anodic current is higher. The wave of the electrocatalytic anodic current starts at the oxidation potential of the polyaniline film, implying that the redox polymer mediates the bioelectrocatalyzed oxidation of glucose by the oxidation of the flavin site in the enzyme.

Knowing the enzyme content in the film, $3 \times 10^{-12} \text{ mol}\cdot\text{cm}^{-2}$, and the highest achieved current density, $i = 0.3 \text{ mA}\cdot\text{cm}^{-2}$, we calculate the electron-transfer turnover rate between the enzyme redox site and the electrode to be ~ 1000 electrons/s. At the temperature employed in our measurements ($\sim 30^\circ \text{C}$), the turnover rate of the native GOx for the electron transfer from glucose to dioxygen (natural electron acceptor) is $\sim 900 \pm 150 \text{ s}^{-1}$.^{30b} The overall rate constant of the bioelectrocatalytic process is estimated⁴⁴ to be $\sim 7.5 \times 10^3 \text{ M}^{-1}\cdot\text{s}^{-1}$. Thus, the reconstituted GOx on the polyaniline/poly(acrylic acid) film reveals a turnover rate similar to that of the native enzyme, implying that the conductive redox polymer provides an extremely efficient electrical contact between the enzyme redox center and the electrode support.

In a control experiment, native GOx was covalently linked to the polyaniline/poly(acrylic acid) film by direct coupling of lysine residues of the biocatalyst to the carboxylic groups in the film. The resulting redox polymer/enzyme assembly shows a minute bioelectrocatalytic current for the oxidation of glucose (~ 2 orders of magnitude lower than the amperometric response of the reconstituted GOx system). This experiment demonstrates that the functionalization of the polymer film with random configurations of the enzyme does not yield an electrically contacted bioelectrocatalytically active matrix. The results emphasize that it is essential to align the enzyme in respect to the polymer film by the reconstitution process. The nanoengineered biocatalytic configuration yields an integrated, electrically contacted assembly.

The bioelectrocatalytic oxidation of glucose by the polyaniline/poly(acrylic acid)/GOx assembly was also characterized by in situ electrochemical-SPR experiments (Figure 4B). Application of the potential corresponding to -0.3 V on the polyaniline/poly(acrylic acid)/GOx-functionalized electrode results in the SPR spectrum shown in Figure 4B, curve a. At this potential, the redox polymer film exists in its reduced state, PAN. Addition of glucose to the system ($E = -0.3 \text{ V}$) results in a change in the SPR spectrum of the film that is independent of the concentration of glucose (Figure 4B, curves b–f). The change in the SPR spectrum of the film is attributed to the reduction of the FAD center in GOx to FADH₂ by the added glucose. The change in the refractive index of the film as a result of the reduction of the FAD site is responsible for the change in the SPR spectra. As all enzyme FAD sites are reduced to the FADH₂ state, independent of the bulk concentration of glucose, the resulting SPR curves are almost identical in the entire range of glucose concentrations. Biasing the potential of the polyaniline/poly(acrylic acid)/GOx electrode at $+0.6 \text{ V}$, in the absence of glucose, results in the SPR spectrum shown in Figure 4(B), curve (a'), that is characteristic of the oxidized polyaniline state, PAN²⁺. Addition of glucose to the system results in a change in the SPR spectra depicted in Figure 4B, curves b'–f'. The minimum reflectivity angle is shifted to lower angles, and the reflectance intensity decreases as the concentration of glucose is elevated. The inset of Figure 4B shows the enlarged SPR spectra measured in the presence of different concentrations of glucose: curves b–f recorded at a potential corresponding to -0.3 V whereas curves b'–f' were recorded at an applied potential of 0.6 V . It can be seen that the SPR spectra of the oxidized polyaniline film shift in their spectral

(42) (a) Yang, C. Y.; Smith, P. Heeger, A. J.; Cao, Y.; Osterholm, J. E. *Polymer* **1994**, *35*, 1142–1147. (b) Palaniappan, S. *Eur. Polym. J.* **2001**, *37*, 975–981.

(43) Hecht, H. J.; Kalisz, H. M.; Hendle, J.; Schmid, R. D.; Schomburg, D. J. *Mol. Biol.* **1993**, *229*, 153–172.

(44) Andrieux, C. P.; Savéant, J. J. *J. Electroanal. Chem.* **1978**, *93*, 163–168.

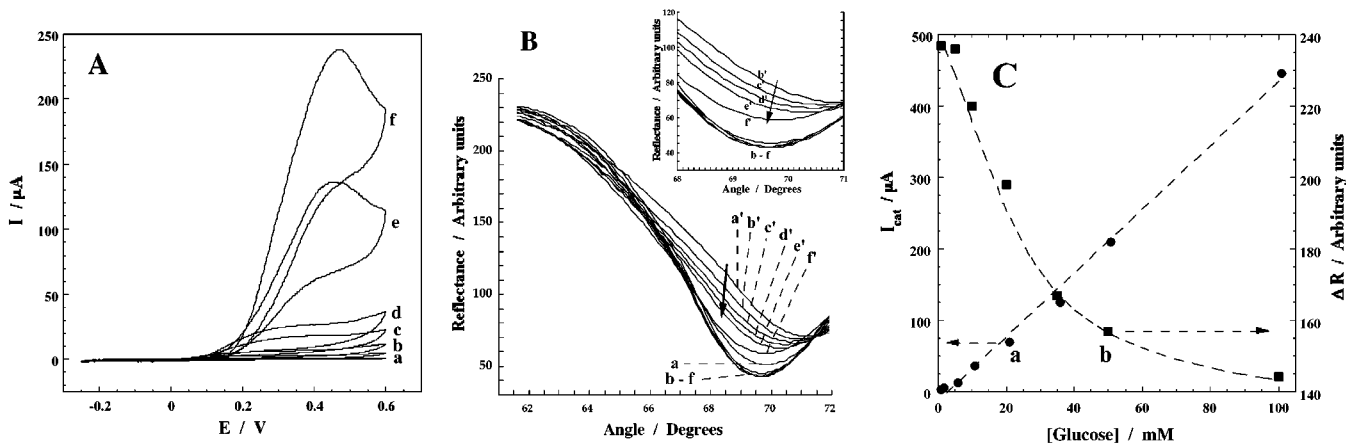


Figure 4. (A) Cyclic voltammograms of the Au electrode modified with the polyaniline/poly(acrylic acid) thin film functionalized with the reconstituted GOx in the presence of various concentrations of glucose: (a) 0, (b) 5, (c) 10, (d) 20, (e) 35, and (f) 50 mM. Potential scan rate, $5 \text{ mV}\cdot\text{s}^{-1}$. (B) SPR spectra of the Au electrode modified with the polyaniline/poly(acrylic acid) thin film and functionalized with the reconstituted glucose oxidase. The spectra depicted in curves a–f were recorded at an applied potential of -0.3 V in the presence of various concentrations of glucose: (a) 0, (b) 5, (c) 10, (d) 20, (e) 35, and (f) 50 mM. The spectra shown in curves a'–f' were recorded at an applied potential of 0.6 V in the presence of various concentrations of glucose: (a') 0, (b') 5, (c') 10, (d') 20, (e') 35, and (f') 50 mM. Inset shows the enlarged SPR spectra. Arrows show the direction of the SPR spectrum shift upon increase of the glucose concentration at the applied potential of 0.6 V . (C) Calibration plots of the amperometric responses, I_{cat} , measured at 0.6 V (a) and changes in the minimum of reflectance intensities ΔR (b) at different concentrations of glucose. The ΔR values were calculated as differences between the reflectance minimum measured at 0.6 V and the reflectance minimum measured at -0.3 V for each glucose concentration. The data were obtained in 0.1 M phosphate buffer, $\text{pH} = 7.0$.

features to those of the reduced film as the concentration of glucose is elevated. This is consistent with the fact that the electron-transfer turnover rate between the enzyme redox site and the electrode is very efficient, and it proves the bioelectrocatalytic mechanism where the polyaniline mediates the oxidation of the enzyme redox center. That is, the electron transfer from the enzyme reduced cofactor, FADH_2 , to the oxidized polymer film, and from it to the Au conductive support (biased at 0.6 V), generates a steady-state ratio $\text{PAN}/\text{PAN}^{2+}$. The content of the reduced polymer state, PAN, in the steady-state population $\text{PAN}/\text{PAN}^{2+}$ is higher as the rate of the electron transfer from FADH_2 to the PAN^{2+} is increased upon elevation of the glucose concentration.

Figure 4C shows the calibration curves derived from the in situ electrochemical-SPR measurements: The amperometric responses of the system (curve a) at different concentrations of glucose are complemented by the changes in the minimum of reflectance intensities, ΔR (curve b). The ΔR values were calculated as the differences between the reflectance minimum measured at 0.6 V and the reflectance minimum measured at -0.3 V for each glucose concentration. We see that the bioelectrocatalytic anodic currents for the oxidation of glucose increase linearly with the elevation of the glucose concentration, whereas the ΔR values reveal a reciprocal dependence upon increasing the concentration of glucose. The origin for the different dependence of the two physical parameters (I_{cat} and ΔR) on the glucose concentration may be quantitatively expressed by kinetic analysis of the electrochemical process in the system. The bioelectrocatalytic oxidation of glucose yields a steady-state ratio of $\text{PAN}/\text{PAN}^{2+}$ in the film. The bioelectrocatalytic current directly relates to the concentration of PAN, leading to a linear dependence of the I_{cat} on the glucose concentration. The ΔR relates, however, to the difference ($[\text{PAN}^{2+}] - [\text{PAN}]$) leading to the reciprocal dependence of ΔR on the glucose concentrations.

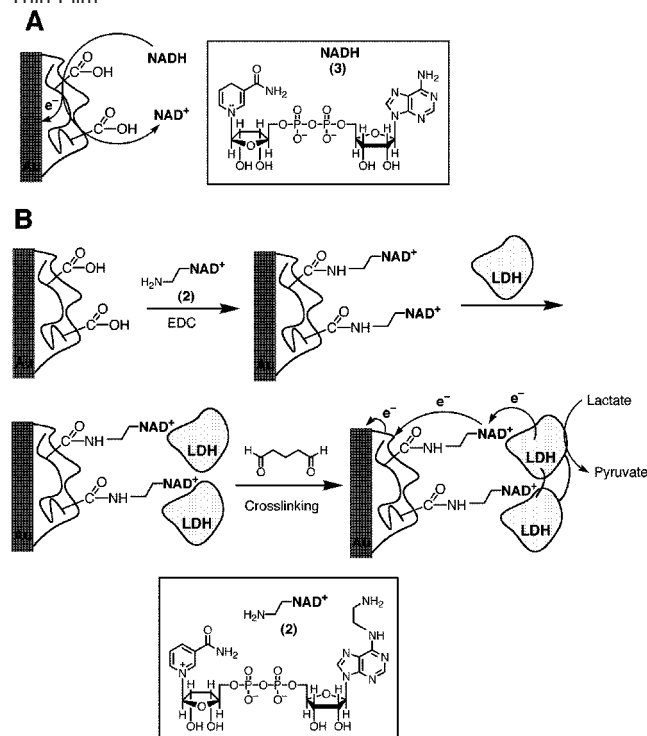
Among the redox enzymes, NAD(P)^+ cofactor-dependent enzymes play a central role. The coupling of NAD(P)^+ -

dependent enzymes with electrodes for bioelectrocatalytic transformations requires the development of electrochemical means for the regeneration of NAD(P)^+ cofactor.^{26,45} The use of NAD(P)^+ -dependent enzymes as bioactive interfaces in sensor devices requires the assembly of the biocatalyst, NAD(P)^+ cofactor, and a cofactor regenerating electrocatalyst as integrated systems that are in electrical contact with the electrode support. The composite polyaniline/poly(acrylic acid) film acts as an electrocatalyst for the oxidation of NADH to NAD^+ ^{36,38} (Scheme 3A). Figure 5A shows the cyclic voltammograms of the polyaniline/poly(acrylic acid)-functionalized electrode at different concentrations of NADH in an in situ electrochemical-SPR experiment. An electrocatalytic anodic current is developed at the oxidation potential of the redox film. The electrocatalytic anodic current increases as the concentration of NADH is elevated. These results imply that the polyaniline film catalyzes the NADH oxidation.

Treatment of the redox polymer-functionalized electrode with different concentrations of NADH , while biasing the electrode at the potential of 0.6 V , would generate a $\text{PAN}/\text{PAN}^{2+}$ steady-state ratio controlled by the rate of the electron transfer from NADH to PAN^{2+} , and this would be controlled by the NADH concentration. While in the absence of NADH the redox polymer will exist at this potential in the PAN^{2+} state, increase of the NADH concentration will elevate the steady-state content of PAN in the $\text{PAN}/\text{PAN}^{2+}$ mixture. Figure 5B shows the SPR spectra of the polyaniline/poly(acrylic acid)-modified electrode in the absence and in the presence of added NADH at two different potentials: at $E = -0.3 \text{ V}$ and at $E = 0.6 \text{ V}$, where the redox polymer is electrochemically reduced and oxidized, respectively. At the potential of -0.3 V , the polymer exists in the PAN state and the spectrum in the absence of NADH is shown in Figure 5B, curve a. Addition of NADH results in a shift in the minimum reflectivity angle to higher values. This change is attributed mainly to the changes in the refractive index

(45) Katakis, I.; Domingues, E. *Mikrochim. Acta* **1997**, *126*, 11–32.

Scheme 3. (A) Electrocatalyzed Oxidation of NADH by the Composite Polyaniline/Poly(acrylic acid) Thin Film. (B) Assembly of the Integrated Lactate Dehydrogenase (LDH) Biocatalytic Interface on the NAD⁺-Functionalized Polyaniline/Poly(acrylic acid) Thin Film



above the polymer–solution interface as a result of the addition of NADH. Theoretical fitting of the spectra reveals that the refractive index changes from $n = 1.338 + 0.008j$ to $n = 1.370 + 0.030j$ upon addition of 10 mM NADH. This change in the refractive index may originate from the association of NADH to the polymer film by multi-H-bond interactions. The shifted SPR spectrum is almost unaffected upon the further addition of NADH (a slight increase in the reflectance intensity, cf. Figure 5B, curves b–d; see also inset). Application of the potential of +0.6 V on the electrode results in the formation of the PAN²⁺ film, and the SPR spectrum in the absence of NADH is shown in Figure 5B, curve a'. The difference between the SPR spectra of the PAN state ($E = -0.3$ V), curve a, and the PAN²⁺ state ($E = 0.6$ V), curve a', originates from the change of the redox polymer refractive index as discussed before. Addition of NADH to the polymer-modified electrode biased at $E = 0.6$ V results in a decrease in the reflectance intensity, and the minimum reflectivity angle is positioned between that of pure PAN²⁺ spectrum and the PAN spectrum. As the concentration of NADH is higher, the spectrum resembles more that of the PAN film, consistent with the fact that the PAN content in the steady-state ratio PAN/PAN²⁺ increases. The inset in Figure 5B shows enlarged spectra of the redox polymer-modified electrode at different concentrations of NADH at $E = -0.3$ V, curves b–d, and at $E = 0.6$ V, curves b'–d'. The SPR spectra recorded at $E = 0.6$ V shift to the pattern of the SPR spectra recorded at $E = -0.3$ V as the concentration of NADH is elevated. Figure 5C shows the calibration curves extracted from the in situ electrochemical-SPR measurements. The amperometric responses of the system (curve a) at different concentrations of NADH are complemented by the changes in the minimum of reflectance intensities, ΔR (curve b). The ΔR

values were calculated as the differences between the reflectance minimum measured at 0.6 V and the reflectance minimum measured at -0.3 V for each of the NADH concentrations.

Our laboratory has reported on the assembly of integrated, electrically contacted, NAD⁺-dependent enzyme electrodes.^{46,30b} The method is based on the assembly of an affinity complex between a NAD⁺-dependent enzyme (e.g., LDH) and a relay-NAD⁺ monolayer, followed by the lateral cross-linking of the surface-associated enzyme to yield a rigid biocatalytic layer. Following this concept, and realizing that PAN²⁺ catalyzes the oxidation of NADH, we use the polyaniline/poly(acrylic acid) as a matrix for the integration and electrical contact of the NAD⁺-dependent enzyme LDH with the electrode support (Scheme 3B). The poly(acrylic acid) included in the polymer film provides anchoring sites for the covalent attachment of 2. Formation of the affinity complex between LDH and the NAD⁺ units,⁴⁷ followed by cross-linking of the LDH components with glutaric dialdehyde, yields the integrated enzyme electrode. Biocatalytic oxidation of lactate to pyruvate in the presence of LDH yields the reduced NADH cofactor that is linked to the polymer matrix. The polymer-mediated oxidation of NADH recycles the cofactor that is further reduced by lactate. The bioelectrocatalytic oxidation of lactate could then be followed by in situ electrochemical-SPR measurements. The polymer-mediated oxidation of NADH should yield an electrocatalytic current, and as the concentration of lactate controls the regeneration efficiency of NADH, the amperometric response of the system should correlate with the concentration of lactate. Furthermore, the application of a potential corresponding to 0.6 V that oxidizes the PAN film to PAN²⁺ will result in a steady-state concentration of PAN/PAN²⁺ that is controlled by the regeneration rate of NADH or the concentration of lactate. The steady-state ratio of PAN/PAN²⁺ can then be followed by SPR spectroscopy. The integrated polyaniline/poly(acrylic acid)/NAD⁺/LDH film was constructed as outlined in Scheme 3B. QCM measurements performed upon the buildup of the biocatalytic functional film on a Au–quartz crystal indicate that the surface coverages of 2 and LDH on the modified surfaces are $\sim 4 \times 10^{-11}$ and $\sim 4 \times 10^{-12}$ mol·cm⁻², respectively.

Figure 6A shows the cyclic voltammograms of the integrated polyaniline/poly(acrylic acid)/NAD⁺/LDH electrode in the presence of different concentrations of lactate. As the concentration of lactate increases, curves b–f, the amperometric response of the electrode is higher. The electrocatalytic currents are observed at the oxidation potential of polyaniline, indicating the redox polymer mediates the oxidation of NADH and the biocatalyzed oxidation of lactate. Knowing the LDH content in the film, 4×10^{-12} mol·cm⁻², and the highest achieved current density, $i = 0.27$ mA·cm⁻², we calculate the electron-transfer turnover rate between the enzyme redox site and the electrode to be ~ 350 s⁻¹. This turnover rate is much lower than that reported for the native LDH operating with diffusional NAD⁺ and lactate (~ 4700 electrons/s).⁴⁸ The overall rate constant of the bioelectrocatalytic process is estimated⁴⁴ to be $\sim 4.7 \times 10^3$ M⁻¹·s⁻¹. This could originate from difficulties for the immobilized NAD⁺ to accommodate the binding sites of the enzyme, thus, resulting

(46) Bardea, A.; Katz, E.; Bückmann, A. F.; Willner, I. *J. Am. Chem. Soc.* **1997**, *119*, 9114–9119.

(47) Kharitonov, A. B.; Alfonta, L.; Katz, E.; Willner, I. *J. Electroanal. Chem.* **2000**, *487*, 133–141.

(48) Eichner, R. D. *Methods Enzymol.* **1982**, *89*, 359–362.

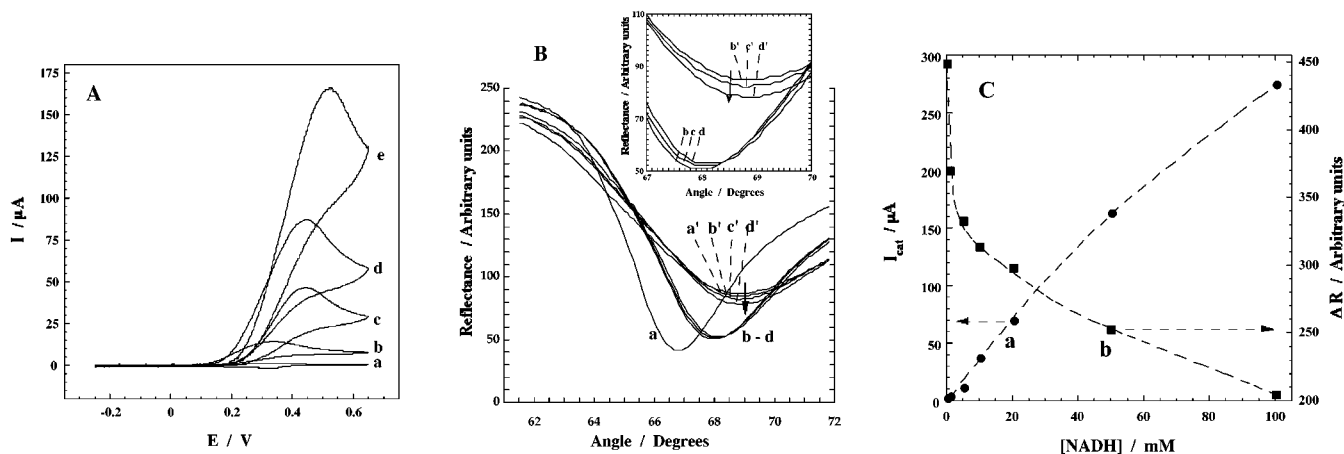


Figure 5. (A) Cyclic voltammograms of the Au electrode modified with the polyaniline/poly(acrylic acid) thin film in the presence of various concentrations of NADH: (a) 0, (b) 10, (c) 20, (d) 50, and (e) 100 mM. Potential scan rate, $5 \text{ mV}\cdot\text{s}^{-1}$. (B) SPR spectra of the Au electrode modified with the polyaniline/poly(acrylic acid) film upon interaction with NADH. The spectra shown in curves a–d were recorded at an applied potential of -0.3 V in the presence of various concentrations of NADH: (a) 0, (b) 5, (c) 10, and (d) 20 mM. The spectra a'–d' were measured upon application of a potential of 0.6 V in the presence of various concentrations of NADH: (a') 0, (b') 5, (c') 10, and (d') 20 mM. Inset shows the enlarged SPR spectra. Arrows show the direction of the SPR spectrum shift upon increase of the NADH concentration at the applied potential of 0.6 V . (C) Calibration plots of the amperometric responses, I_{cat} , measured at an applied potential of 0.6 V (a) and the respective changes in the minimum of reflectance intensities ΔR (b) at different concentrations of NADH. The ΔR values were calculated as differences between the reflectance minimum measured at 0.6 V and the reflectance minimum measured at -0.3 V for each NADH concentration. The data were obtained in 0.1 M phosphate buffer, $\text{pH} = 7.0$.

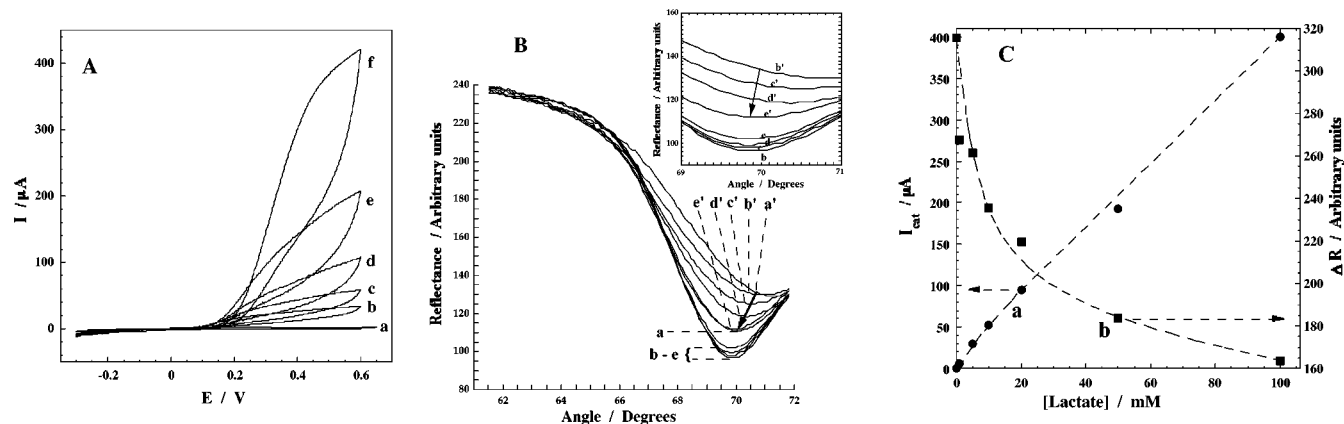


Figure 6. (A) Cyclic voltammograms of the Au electrode modified with the polyaniline/poly(acrylic acid) film and functionalized with the NAD^+ cofactor units and the cross-linked LDH in the presence of various concentrations of lactate: (a) 0, (b) 5, (c) 10, (d) 20, (e) 50, and (f) 100 mM. Potential scan rate, $5 \text{ mV}\cdot\text{s}^{-1}$. (B) SPR spectra of the Au electrode modified with the polyaniline/poly(acrylic acid) film and functionalized with the NAD^+ cofactor units and the cross-linked LDH. The spectra shown in curves a–e were recorded at an applied potential of -0.3 V in the presence of various concentrations of lactate: (a) 0, (b) 1, (c) 5, (d) 10, and (e) 20 mM. The spectra depicted in curves a'–e' were recorded at an applied potential of 0.6 V in the presence of various concentrations of lactate: (a') 0, (b') 1, (c') 5, (d') 10, and (e') 20 mM. Inset shows the enlarged SPR spectra. Arrows show the direction of the SPR spectrum shift upon increase of the lactate concentration and at an applied potential of 0.6 V . (C) Calibration plots of the amperometric responses, I_{cat} , measured at an applied potential of 0.6 V (a) and changes in the minimum of reflectance intensities ΔR (b) at different concentrations of lactate. The ΔR values were calculated as differences between the reflectance minimum measured at 0.6 V and the reflectance minimum measured at -0.3 V for each lactate concentration. The data were obtained in 0.1 M phosphate buffer, $\text{pH} = 7.0$.

in nonoptimized positions of the cofactor units in the biocatalytic enzyme/cofactor assembly.

The electrochemically induced biocatalyzed oxidation of lactate can be nicely followed by the SPR spectroscopy (Figure 6B). At a potential of -0.3 V applied on the integrated biocatalytic electrode, where the polymer film exists in the PAN state, addition of lactate results in a decrease in the minimum reflectivity angle (cf. Figure 6B, the shift of curve a to curve b). The SPR spectrum angle of the polymer is almost unaffected by the concentration of lactate, and the SPR spectra at 1×10^{-3} and $2 \times 10^{-2} \text{ M}$ lactate are almost identical. This is consistent with the fact that the addition of lactate to the integrated electrode existing in the PAN state, results in the reduction of the immobilized NAD^+ to NADH. The change in the refractive

index of the film originating from the biocatalyzed reduction of NAD^+ to NADH results in the decrease in the minimum reflectivity angle. As the low concentration of added lactate is sufficient to reduce all of the NAD^+ units associated with the film, the SPR spectrum of the redox film-modified electrode is independent of the concentration of lactate. Biasing the potential of the polyaniline/poly(acrylic acid)/ NAD^+ /LDH electrode at 0.6 V in the absence of lactate results in the SPR spectrum shown in Figure 6B, curve a'. Addition of lactate to the electrode results in the changes in the SPR spectrum shown in Figure 6B, curves b'–e' (see also the inset). The minimum reflectivities of the SPR spectra decrease in their intensities and the minimum reflectivity angles are shifted to lower values as the lactate concentration increases. That is, as the concentration of lactate

increases, the SPR spectra resemble more the spectrum of the reduced assembly that includes the PAn state rather than the oxidized PAn²⁺ state even though the potential applied on the electrode corresponds to 0.6 V. This is consistent with the mechanism of the biocatalytic oxidation of lactate, where the polyaniline layer mediates the electron transfer from the immobilized NADH units to the electrode conductive support. Thus, increase of the lactate concentration enhances the rate of NADH formation. As a result, the content of PAn state in the steady-state ratio of PAn/PAn²⁺ is higher as the lactate concentration increases, leading to the observed changes in the SPR spectra. Figure 6C shows the respective calibration curves corresponding to the in situ electrochemical-SPR analysis of lactic acid. The changes in the reflectivity intensities, ΔR , at variable concentrations of lactate are depicted in parallel to the amperometric responses of the system at the respective concentrations of lactate.

The final aspect to consider relates to the stability of the resulting integrated enzyme electrodes. We found that the GOx-reconstituted PAn film-functionalized electrode is stable upon storage at 4 °C for at least 1 month (residual activity >95%). The electrodes reveal an activity decrease of ~5% upon continuous operation at room temperature for 24 h. The NAD⁺/LDH/PAn integrated electrode shows 90% of its original activity after storage at 4 °C for 1 month, and loses ~10% of its activity upon continuous operation for 12 h at room temperature.

Conclusions

An electrochemical method to polymerize a polyaniline/poly(acrylic acid) composite film on SPR electrodes was developed. The incorporation of poly(acrylic acid) in the polyaniline film shifted the redox functions of the film to a neutral pH (pH =

7.0). SPR measurements allowed the optical transduction of the redox-switching functions of the polymer and enabled the characterization of the dynamics of swelling of the oxidized film, PAn²⁺ state, and of the shrinking of the reduced polymer, PAn state, upon the cyclic redox processes, respectively.

The redox activity of the polymer film at neutral pH values allows the coupling of redox biocatalysts to the electrochemical functions of PAn. The coassembled poly(acrylic acid) units provide binding sites for covalent attachment of the enzyme cofactors (FAD or NAD⁺ amino derivatives) to the polymer film and subsequently the association of the biocatalysts (GOx or LDH, respectively) on the cofactor-functionalized electrodes, to yield integrated, electrically contacted bioelectrocatalytic assemblies. In situ electrochemical-SPR measurements enabled us to transduce the bioelectrocatalytic functions of the enzyme-modified film by amperometric or optical means.

Recently, we reported on the electrochemically induced micromechanical movement of a polyaniline-functionalized Au-coated cantilever, at pH = 2, using controlled surface-induced electrostatic stress interactions.^{5b} The present study shifts the polyaniline redox activity to neutral pH values and the biocatalysts integrated in the polymer films control the PAn/PAn²⁺ ratio by means of the respective biocatalyzed transformations. Thus, control of the electrostatic repulsions or surface stress interactions on microobjects by bioelectrocatalytic transformations could lead in the future to biomaterial-based micromechanical sensors or micromechanical actuators.

Acknowledgment. This research was supported by the ATOMS EC grant.

JA012680R